Strain Sensing Comparison Between Single and Multimode Fibers using Optical Low Coherence Interferometry

Nafiul Matiin[1] and Shih-Hsiang Hsu[2]

Abstract— **Optical low coherence interferometry is one of the accurate optical sensing technologies and widely utilized in various physical sensing properties. The system principle is to characterize the relative interferogram movement distance caused by the various strain on a sensing arm. An interferometric strain sensor from two-stage Mach-Zehnder interferometer was demonstrated for double sensitivity improvement. The strain performance comparison between single and multimode fibers will be analyzed for fiber sensing applications. The stepper motor was set up with a movement distance of 20 nm in every step and the velocity could achieve 10000 step/s. The fiber strain was characterized as 22.22 με on a 9-cm length. The experimental results demonstrated the multimode fiber sensitivity is higher than single mode fiber. Repeatability of both single and multimode are uncertain. The interferogram movement distance from the multimode fiber was higher than a single mode and demonstrates higher sensitivity.**

Keywords— **FLRD, Low Coherence Interferometry, Strain Sensor**

I. INTRODUCTION

Fiber optics has undoubtedly had profound impact on the communications industry. It is based on the theory that optical signals could be transmitted along glass or silica fibers with a loss potentially below that experienced in coaxial copper cables. Further, unlike copper where skin effect increases loss with baseband modulation frequency, the loss in optical fibers could be maintained for all conceivable modulation frequencies. But in 1965, glass fibers had already appeared in ornamental lamps and the basic ideas of the dielectric waveguide were well establish. Using optical fibers to guide light to and from a place at which a measurement was to be made had already emerged and had gone from concept to practice. From the early beginnings almost 35 years ago, the Optical Fiber Sensor (OFS) community became infected with communications euphoria, and by the mid 1970s to the early 1980s felt OFS technology was the solution to everything. Realism percolated, though perhaps a little slow, and now we know that there are areas of real application, but that there are still interesting and relevant problems left to excite the research community. Fiber Optic Sensor (FOS) technology had been developed in 1980s, and continued progress to the present time.

[1]Nafi'ul Matiin is with Departement of Engineering Physics, Faculty of Technology Industry, Institut Teknologi Sepuluh Nopember, Surabaya, 60111. E-mail : nafitint77@gmail.com.

[2]Shih-Hsiang Hsu Mentari is with Departement of Graduate Institute of Electro-Optical Engineering, Faculty of Electrical Engineering and Computer Science, National Taiwan University of Science and Technology, Taiwan. E-mail: shsu@mail.ntust.edu.tw.

The motivation of the study is because FOS has many advantages such ; light weight, small footprint, immunity to electromagnetic interference, easily multiplexable (for multiple function or single function in multiple sensing locations), require no electrical power at the sensing point, and in most cases have the potential to be produced at low cost. FOS technology have been studied over three decades and have involve several round of revolutionary change with advances in light source, fiber optics, and spectroscopy methods. Due to the diversity of the quantities (measurer or parameters), a variety of sensing mechanisms has been investigated to improve performance on either one or all of the basic merits of sensitivity, selectivity, accuracy, reliability, and robustness. To date, various sensing mechanisms have been established for individual sensors and will remain largely unchanged in next several years [1-6].

LCI has been proposed and studied since the beginning of the optical science. However, for the last 20 year, there has been a dramatically increase in its applications, mainly due to the development of optical coherence tomography and the evolution of new light sources. The first works of in surface and optical material characterization was reported in 1960. In 80's some applications in fiber optics characterization [7], topography surfaces and internal structures in transparent media [8] were proposed with a LCI set up. It is generally accepted that first biological application was reported by Fercher [9]. After these first works, Optical Coherence Tomography (OCT) became a powerful technique for medical diagnosis, in which image of the human retina and coronary artery were obtained [10]. Since then, OCT has evolved, and nowadays it is a well

established technique for ophthalmic diagnosis and other biological tissues [11].

Strain sensor based on interferometry system was demonstrated in some research [12, 13, 14]. Mach-Zehnder optical fiber interferometric sensor is used to measure the dynamic strain of a vibrating cantilever beam [15]. This used demodulation of the phase shift that has advantage of passive detection and low cost as it requires no phase or frequency modulation in reference arm. Another technology of Mach-Zehnder strain sensor is used displacement sensing principle, that the applied strain causes the variation of light intensity in two ways [13]. First, the strained fiber of the main branch of a Mach-Zehnder interferometer exhibits length variation, so the superposed light intensity at the output of Mach-Zehnder interferometer is proportional to the strain. This variation of intensity due to the phase shift results from the elongation of the fiber. Second, the length variation in fiber reduces the distance between the head of the fiber and the fixed mirror which is turn leads to intensity variation of the light. Fiber grating are also used widely as fiber strain sensing [16, 17]. Fiber Bragg Grating (FBG) are increasingly being used in sensing applications and are enjoying widespread acceptance and used. The FBG is an optical filtering device that reflects light of a specific wavelength and is present within the core of an optical fiber waveguide. These sensors are particularly attractive for quasi distributed sensing, as many gratings can be written into a length of fiber and addressed using either wavelength division or time division multiplexing. Various sensing scheme typically involving the use of several grating sensors located along a fiber path, or in a star type of arrangement. The system is illuminated using a broadband source, such as an edge emitting LED, superluminescent diode, or superfluorescent fiber source, and each grating in the system return a narrow band wavelength component. The grating wavelengths all fall within the bandwidth of the source. Measurand induced perturbation of an individual grating in the system change the wavelength returned by that specific element, which can be detected at the output and then related to the measurand at that sensor position. The wavelength encoded nature of the output has a number of distinct advantages over direct intensity based sensing schemes, most importantly, the self referencing nature of the output. The sensed information is encoded directly into wavelength, which is an absolute parameter and does not depend on the total light level, losses in the connecting fibers and couplers, or source power.

Optical Low Coherence Interferometry (OLCI) is the one of the most popular sensing technologies that can be utilized to precisely gauge various physical sensing properties, such as temperature, pressure, force, strain, positioning, vibration, and refractive index using interferograms [18]. As strain sensor, two stages optical low coherence Mach-Zehnder interferometry will be demonstrated. The strain performance comparison between single and multimode fibers will be analyzed for fiber sensing applications.

II. Literature Review

A. *Low Coherence Interferometry Principle*

Low coherence interferometry is a special kind of interferometry. Instead of strongly coherent monochromatic light, broadband or ultrashort pulse light with a short coherence length is used. Contrary to interferometry with monochromatic light, the short coherence length of broadband light defines an additional absolute reference. This mean that interference between two waves is possible only if the path length difference is smaller than the coherence length. Thus LCI has found a wide range of technical applications, i.e., in biomedical imaging or topographical surface analysis, and is today often knows as Optical Coherence Tomography (OCT).

Low coherence interferometry basically does not differ in the design of the optical components from a classical interferometer [19]. Only the monochromatic and coherent light source is replaced by a light source with certain short coherent light pulses. A very common and simple example to study principle of interferometer is the Michelson type that describe in figure 1. The basic building block is a light source, a detector, two mirrors and one semitransparent mirror (beam splitter).

Consider the upper mirror that figure, where the distance $d_r = 2l_r$ to the beam splitter is known. The right mirror instead is located at an unknown distance d. the reference mirror can be move back or forth until interference occurs. Since interference (twice the distance to the beam splitter) of the reference and second mirror is within the coherence length of the light source, the position of the second mirror is hence known by the position of the reference mirror. (See figure 1).

$$d = d_r \quad (1)$$

$$|(d - d_r)| = 2|(l - l_r)| < l_c \quad (2)$$

Replacing the second mirror by an object to be investigated, gives rise to various LCI applications such as, for example surface profilometry.

B. *Mach Zehnder Interferometer*

In this research, dataset (tweet) was collected from Twitter. The tweets were crawled based on keyword from name list of public figure that refers to Litbang Kompas survey [8]. The public figures were related to Indonesian election for 2014. There are six names used in this research from popular public figure. They are Aburizal Bakrie, Dahlan Iskan, Gita Wirjawan, Joko Widodo, Prabowo Subianto, and Rhoma Irama.

Mach-Zehnder interferometer is a particularly simple device for demonstrating interference by division of amplitude. A light beam is first split into two parts by a beam splitter and then recombined by a second beam splitter. Depending on the relative phase acquired by the beam along the two paths the second beam splitter will reflect the beam with efficiency between 1 and 100%. The schematic diagram of a Mach-Zehnder interferometer is shown in figure x. It consist of two 2 x 2 couplers at the input and output. The excitation is applied to the sensing fiber, resulting optical path difference between the reference and sensing fibers. The

light intensity of the output of the Mach-Zehnder interferometer can be expressed as:

$$I = 2A^2(1 + \cos\Delta\phi) \quad (3)$$

$$\Delta\phi = \frac{2\pi n_o}{\lambda}\left\{1 - \frac{n_o}{2}[(1-v)p_{12} - v_f p_{11}]\right\}\int_{L_f} \varepsilon_f \, dx \quad (4)$$

where, $\Delta\phi$ is the phase shift, n_o is the refractive index of the optical fiber, λ is the optical wavelength, v_f is the Poisson's ratio, p_{11} and p_{12} are the Pockel's constant, L_f and ε_f are the length and strain of the optical fiber, respectively. Since the term in front of the integral are constant for any given optical fiber system, the total optical phase shift $\Delta\phi$ is proportional to the integral of the optical fiber strain. By measuring the total optical phase shift, the integral of the optical fiber strain can be obtained as follows :

$$\int_{\Gamma_s} \varepsilon_f dx = \frac{\Delta\phi}{\frac{2\pi n_o}{\lambda}\left\{1 - \frac{n_o^2}{2}[(1-v)p_{12} - v_f p_{11}]\right\}} \quad (5)$$

C. *Fiber Optic Strain Gauge*

Introducing different strain in the two fibers causes a difference in optical path lengths and, hence, motion of the fringes. This phenomenon serves as a sensitive fiber optic strain gauge. If one or both fibers are attached to a structure which is then strained under load, the strain in that structure can be determined from the motion of the optical interference fringes.

To calculate the expected fringe shift due to longitudinal strain, let the section of single mode fiber to be strained be of length L with its axis in the x direction. The propagation constant of the mode in the fiber is designated by β, its free space propagation constant is k_o, the fiber core index is n, the core diameter is D, and poisson's ratio for the fiber material is μ. The phase of the light wave after going through this fiber section can be determine by :

$$\phi = \beta L \quad (6)$$

The change in ϕ due to physical change of length (ΔL) produced by the strain is simply determined by :

$$\beta\Delta L = \beta\varepsilon L \quad (7)$$

The other term is the change in ϕ due to change in β, can come from two effect; the strain optics effects whereby the strain changes the refractive index of the fiber, and waveguide mode dispersion effect due to a change in fiber diameter D produced by longitudinal strain [46/20].

$$L\Delta\beta = L\frac{d\beta}{dn}\Delta n + L\frac{d\beta}{dD}\Delta D \quad (8)$$

Although $\beta = n_{eff}k_o$, where the effective index n_{eff} lies between core and cladding indices, these indices typically only differ by the other of 1% so we can use $\beta \cong nk_o$. Thus, $d\beta/dn = k_o = \beta/n$. The strain optics effect appears as a change in the optical indicatrix

$$\Delta\left(\frac{1}{n^2}\right)_i = \sum_{j=1}^{6} p_{ij}S_j \quad (9)$$

where S_j is the strain vector, p_{ij} is the strain optic tensor, and the subscripts are in the standard contracted notation. For longitudinal strain in the x direction as considered here, the strain vector is :

$$S_j = \begin{bmatrix} \epsilon \\ -\mu\epsilon \\ -\mu\epsilon \\ 0 \\ 0 \\ 0 \end{bmatrix} \quad (10)$$

For a homogeneous isotropic medium, p_{ij} has only two numerical values, designated p_{11} and p_{12}, and the change in the optical indicatrix in the y and z direction sees an index change :

$$\Delta n = -\frac{1}{2}n^3\Delta\left(\frac{1}{n^2}\right)_{2,3} = -\frac{1}{2}n^3[\epsilon(1-\mu)p_{12} - \mu\epsilon p_{11}] \quad (11)$$

The change of diameter (ΔD) will affect the change in the waveguide mode propagation constant. The change diameter formula is just $\Delta D = \mu\epsilon D$. The $d\beta/dD$ term can be evaluated using the normalized parameters b and V describing the waveguide mode. It can be shown that :

$$\frac{d\beta}{dB} = \frac{\left(\frac{V^3}{2\beta D^3}\right)db}{dV} \quad (12)$$

where, db/dV is the slope of the b – V dispersion curve at the point which describes the waveguide mode. This term will be shown to be negligible. The phase change per unit stress per unit fiber length than can be determine by combining equation above become;

$$\frac{\Delta\phi}{\epsilon L} = \beta - \frac{1}{2}\beta n^2[(1-\mu)p_{12} - \mu p_{11}] + \frac{V^3\mu}{2\beta D^2}\frac{db}{dV} \quad (13)$$

The effect of waveguide mode dispersion is negligible, and so that term can be dropped, giving the simplified expression:

$$\frac{\Delta\phi}{\epsilon L} = \beta - \frac{1}{2}\beta n^2[(1-\mu)p_{12} - \mu p_{11}] \quad (14)$$

By measuring the phase change of light propagating through the fiber due to a longitudinal strain, it is possible to determine the individual values of the two coefficients p_{11} and p_{12}. Using first order theory of elasticity and the photoelastic effect, and assuming that the fiber is elastic and mechanically homogeneous, the phase change $\Delta\phi$ induced by an elongation ΔL is given by [20].

$$\Delta\phi = k[n\Delta L + \Delta n L] = kn\Delta L\{1 - (n^2/2)[p_{12} - v(p_{11} + p_{12})]\} \quad (15)$$

where, $k = 2\pi/\lambda$ denotes the free space wave number, λ is the wavelength, n is the refractive index, Δn is refractive index change, and v is the Poisson's ratio of the fiber material. This equation shows that the optical phase is modified due to change in both the physical of the fiber and the refractive index. The influence due to a change in the fiber diameter (waveguide geometry effect) is small and can therefore be neglected.

III. METHODOLOGY

A. *Design*

In this research, optical low coherence MZ interferometry system with a low coherence broadband light source was used to illustrate the phase matching using two staged optical MZ interferometers by the movable arm through optical collimator scanning, as shown in figure 2. The first MZ interferometer was used for sensing and the second was utilized to analyze the

strain effect. The optical path difference between two MZ arms in the first stage was defined as:

$$\Delta L_1 = L_a - L_b \quad (16)$$

$$\Delta L_2 = L_c - L_d \quad (17)$$

ΔL_2 was movable, representing the phase difference in the second stage.

Once the strain is applied on the sensing arm, the central maximum remains the same position and two side maximum interferograms will move away from the center position. The relationship between phase change $\Delta\phi$ and elongation ΔL is given by the equation:

$$\Delta\phi = k[n_{fiber}\Delta L + \Delta n_{fiber} L] = n_{fiber} kL\left(\frac{\Delta L}{L} + \frac{\Delta n_{fiber}}{n_{fiber}}\right) \quad (18)$$

$$\Delta\phi = kn_{fiber}\Delta L\{1 - (n_{fiber}{}^2/2)[p_{12} - v(p_{11} + p_{12})]\} = kn_{fiber}\Delta L\xi \quad (19)$$

where L is the total fiber length, k is wave number, n_{fiber} is fiber refractive index, Δn_{fiber} and ΔL are variation from fiber refractive index and fiber length difference on MZ interferometer arms, respectively. P_{ij} is pockels coefficient, and v is poisson's ratio of the fiber materials, ξ is the strain optic correction factor.

Following equation (19), the phase detection from the fiber strain variation in the interferometer can be listed as follow:

$$\Delta\phi = (0.79 n_{fiber}\Delta L)k = L_{MD}k \quad (20)$$

where L_{MD} is length of movement distance. In a typical fused silica fiber, v = 0.16, n_{fiber} = 1.46, p_{11} = 0.113, p_{12} = 0.252, and ξ = 0.79, which accounts for the sensitivity reduction due to the stress optic effect on silica fiber material [13].

The first MZ interferometer was used for sensing and the second was utilized to analyze the strain effect. The optical path difference between two MZ arms in the first stage was defined as ΔL_1 and the ΔL_2 was movable, representing the phase difference in the first stage. The output optical intensity (I_o) from the constant ΔL_1 and movable collimator position, ΔL_2, can be described as follows:

$$I_o \propto 2\exp\left\{-\frac{1}{2}(k\Delta L_2)^2\right\} + \exp\left\{-\frac{1}{2}[k(\Delta L_2 + \Delta L_1)^2]\right\} + \exp\left\{-\frac{1}{2}[k(\Delta L_2 - \Delta L_1)^2]\right\} \quad (21)$$

The interferogram movement distance in the first reference MZ stage was characterized as L_{MD2} by optical collimator scanning, the similar situation applied to the first stage as L_{MD1}. The strain value ε of an axially loaded fiber is expressed as the ratio of the sensing length change, ΔL_1, to the original fiber length L and can be written as $\Delta L_1/L$ ($\varepsilon = \Delta L_1/L$). The optical intensity relative to the movable collimator positions represented the interferograms for three kind of optical path differences through two movable collimators. As shown in figure 4.2, the optical intensity maxima are located at: $\Delta L_2 = 0$, $\Delta L_2 = \Delta L_1$, and $\Delta L_2 = -\Delta L_1$ with the high coherence length light source interferogram employing a stable continuous waveform. The sensitivity S in this system can be expressed in the following [13]:

$$L_{MD1} = 0.79 n_{fiber}\Delta L_1 \quad (22)$$

$$L_{MD2} = 0.79 n_{fiber}(-\Delta L_2) \quad (23)$$

$$S = \frac{L_{MD1} - L_{MD2}}{\varepsilon} = 1.58 n_{fiber} L \quad (24)$$

where the factor 2 comes from the double optical path difference and n_{fiber} is the refractive index of a single mode SMF-28 fiber.

B. *Experimental Method*

Methodology of the experimental are showed in the figure 4. Explanation of the flowchart is as follow :

1. Setting up the interferometry system which include: fiber strain path, stepper motor, fiber coupler and connection, and lab view program (for display).
2. Input parameter in lab view program. To get interferogram pattern at the first time, data points were plotted in: 10000 point in 1 second and 1 point equal to 20 nm movement (of movable arm).
3. Run the system with SLED as broadband source, and observe interferogram pattern that show on the PC/display.
4. When interferogram pattern appear, stopped stepper motor and give strain in the sensing arm. In the sensing arm, length of fiber (L) is 9 cm and length change in one step is 2 μm. So, strain in every step: ε = ΔL/L = 22.22 με.
5. Observe interferogram pattern after strain were applied. Accordance to the theoretical, interferogram movement distance will be longer than before.
6. Strain applied in the sensing arm in several steps (each step = 22.22 με).
7. Single mode and multi mode fiber used in sensing arm to analyzed for fiber sensing application.

IV. Result and Discussion

A. *Setting Interferometer System*

In sensing part, fiber strain path built with fiber that clipped on two holders. One side is fix, and another is movable (see figure 5). Fiber pulled in several steps with every step is 2 μm pulled. The original length of fiber was pulled is 9 cm. So, the strain value of every step can be calculated as :

$$\varepsilon = \frac{\Delta L}{L} = \frac{2\,x\,10^{-6}}{9\,x\,10^{-2}} = 22.22\,\mu\varepsilon \quad (22)$$

Single mode and multimode fiber with same parameter (length and refractive index) are used in sensing path and would be analyzed.

Before do strain measurement, two stages MZ interferometry system was tested to find interferogram pattern. This step does by running the motor stepper and observed interferogram pattern. Figure 6 show movable arm of second stages MZ interferometry. Collimator movement distance implemented with the effective index of the optical path in MZ arms was representing the interferogram movement distance different. This collimator scanning will be demonstrated three peak interferogram.

To illustrate the result developed in this work, we apply the proposed method to solve the following numerical examples (See Figure 7.).

The motor stepper setting up with movement distance 20 nm in every step and the velocity 10000 step/s. Time

scanning for this stepper to find three maximum peaks of interferograms was 120 second when sensing path use SMF and 260 second when sensing path use MMF. Figure 7 show interferogram pattern MZ interferometry system without strain. The figure show that, interferogram distance of MMF is higher than SMF. This is indicated that loss transmission and the noise of multimode fiber is higher.

B. Strain Measurement

Strain measurement with low coherence MZ interferometer done with two stage of MZ interferometry system. As explained in the previous part, this system built with the single mode and multimode fiber sensing arm and strain will given by pulling fiber in several step. Length of the fiber that was pulling is 9 cm and refractive index is 1.46. From equation (4.4) in chapter 4, sensitivity of the system will become:

$$S = \frac{L_{MD1} - L_{MD2}}{\varepsilon} = 1.58 n_{eff} L$$

$$S = 1.58 \text{ x } 1.46 \text{ x } 9 \text{ cm} = 0.21 \ \mu m/\mu\varepsilon$$

So, with the specified parameters, sensitivity of the system theoretically is 0.21μm/με.

Single mode fiber used as sensing arm in the MZ interferometer system. Fiber pulled 5-7 times with every step gives ΔL = 2 μm. The strain measurement repeated two times to analyze repeatability of the sensor.

From figure 8, sensitivity of the system with single mode fiber is 0.5 μm/με in the first measurement and increase to 0.3μm/με in the second measurement. Two chart is high in linearity of the strain value and moving distance.

Similar with single mode fiber, multimode fiber that used as sensing arm is 9 cm length and pulled with every step = 2 μm. This fiber pulled 4 – 5 times (less than single mode fiber) because multimode performance is more fluctuating than single mode and this kind of fiber has many peak, so for the observation is more difficult.

Figure 9. show performance of multimode fiber as strain sensor. From that figure, sensitivity of the sensor is 0.8μm/με for firs measurement and 0.4μm/με for second measurement. Linearity of multimode fiber is higher than single mode. Repeatability also shows better than single mode.

Repeatability of both single and multimode is uncertain according trendline of the chart. But in single mode, after it strained even it return in original condition, moving distance is change high (in first pulling). But for next step has the same response than first measurement. Compared with several researches about interferometer for strain sensor, its demonstrate that sensitivity of the system is around 1 μm/με [49,59,60/22, 23, 24]. According to that, sensitivity of this system is lower caused by different length of fiber (length fiber of this system is 9 cm and other research in meters unit).

V. CONCLUSION

A. Conclusion

Strain sensing comparison between single and multimode fibers using optical low coherence interferometry has been demonstrated. Two stages Mach-Zehnder interferometry with sensing arm in the first stage and analyzing parts with stepper motor in the second stage used for strain sensing structure has been completed. Motor stepper setting up with movement distance 20 nm in every step and the velocity 10000 step/s. Strain given on the fiber is 22.22 με in 9 cm of original length and it is applied several times.

According to experimental result, the sensitivity of multimode fiber is higher than single mode fiber, but multimode is unstable and high fluctuation that cause could not measure strain in many point. Repeatability of both single and multimode are uncertain and the system needs to be evaluated. Interferogram distance of MMF is higher than SMF, that indicated the loss transmission and the noise of multimode fiber is higher

B. Future Work

Although low coherence MZ interferometry as strain sensor with single and multimode fiber in sensing arm has been demonstrated, further understanding for structure parameter on performance need to be proposed. In recent thesis, sensitivity of sensor system is around 10^{-1} μm/ με. This sensitivity can be enhanced by increasing length of fiber. And for uncertain of the output performance, evaluation of the system needs to be improved by increasing repetition number of measurement. In the future, low coherence interferometry for sensing other parameters such as temperature and pressure should be proposed.

REFERENCES

[1] Brian Culshaw, "Fiber-Optic Sensing: A Historical Perspective," *Journal of Lightwave Technology*, vol. 26, no. 9, pp. 1064-1078, May 2008.

[2] Brian Chusaw, "Fiber Optics in Sensing and Measurement," *IEEE Journal of Selected Topics in Quantum Electronics*, vol. 6, no. 6, pp. 1014-1021, Nov-Dec 2000.

[3] J W Berthold, "Historical of Microbend Fiber-Optic Sensors," *Journal of Lightwave Technology*, vol. 13, no. 7, pp. 1193-1199, July 1995.

[4] K Fidanboylu and H S Efendioglu, "Fiber Optic Sensor and Their Applications," in *5th International Advanced Technologies Symposium (IATS'09)*, Karabuk, 2009, pp. 1-6.

[5] V. G M Annamdas, "Review on Developments in Fiber Optical Sensors and Applications," *International Journal of Materials Engineering*, vol. 1, no. 1, pp. 1-16, 2011.

[6] Alan D Kersey, "A Review of Recent Developments in Fiber Optic Sensor Technology," *Optical Fiber Technology*, vol. 2, no. 3, pp. 291-317, July 1996.

[7] K Takada, I Yokohama, K Chida, and J Noda, "New Measurement System for Fault Location in Optical Waveguide Devices Based on An Interferometric Technique," *Applied Optics*, vol. 26, no. 9, pp. 1603-1606, May 1987.

[8] R Leitgeb, C Hitzenberger, and Adolf Fercher, "Performance of Fourier Domain vs. Time Domain Optical Coherence Tomography," *Optics Express*, vol. 11, no. 8, pp. 889-894, April 2003.

[9] D Huang et al., "Optical Coherence Tomography," *Science*, vol. 254, no. 5035, pp. 1178-1181, November 1991.

[10] T Bajraszewski et al., "Improved Spectral Optical Coherence Tomography using Optical Frequency Comb," *Optics Express*, vol. 16, no. 6, pp. 4163-4176, March 2008.
[11] S C Her and C M Yang, "Dynamic Strain Measured by Mach-Zehnder Interferometric Optical Fiber Sensors," *Sensors*, vol. 12, no. 3, pp. 3314-3326, March 2012.
[12] N. M S Jahed, T Nurmohammadi, S Ounie, and R S Bonabi, "Enhanced Resolution Fiber Optic Strain Sensor Based on Mach-Zehnder Interferometer and Displacement Sensing Principles," in *International Conference on Electrical and Electronics Engineering (ELECO)*, Bursa, Turkey, 2009, pp. II-302 - II-306.
[13] C D Butter and G B Hocker, "Fiber Optics Strain Gauge," *Applied Optics*, vol. 17, no. 18, pp. 2867-2869, September 1978.
[14] A D Kersey, T A Berkoff, and W W Morey, "High-Resolution Fibre-Grating Based Strain Sensor with Interferometric Wavelength-Shift Detection," *Electronics Letters*, vol. 28, no. 3, pp. 236-238, January 1992.
[15] Y J Rao and David A Jackson, "and , "Recent Progress in Fibre Optic Low-Coherence Interferometry," *Measurement Science and Technology*, vol. 7, no. 7, pp. 981-999, JUly 1996.
[16] A Kempe, "Low Coherence Interferometry In Turbomachinery and Flow Velocimetry," Swiss Federal Institute of Technology, Zurich, PhD Thesis 2007.
[17] A Bertholds and R Dandliker, "Determination of the Individual Strain-Optic Coefficients in Single-Mode Optical Fibers," *Lightwave Technology*, vol. 6, no. 1, pp. 17-20, January 1988.

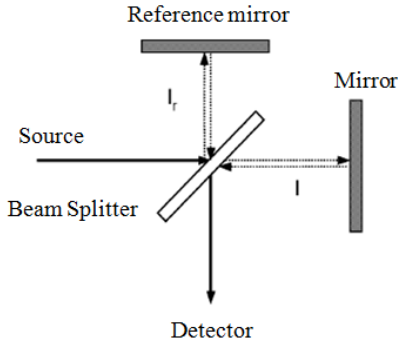

Figure 1. Basic Principle of Michelson Interferometer.

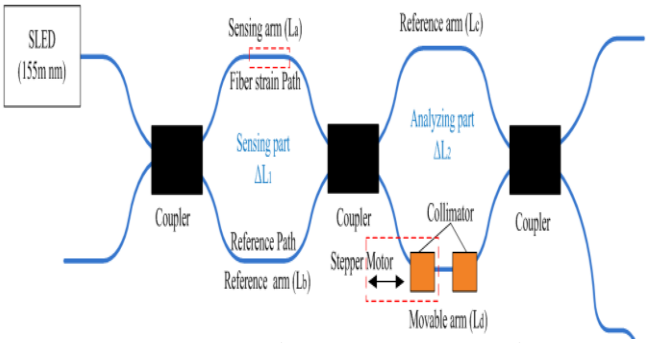

Figure 2. Schematic diagram of two stage optical MZ interferometer strain sensor

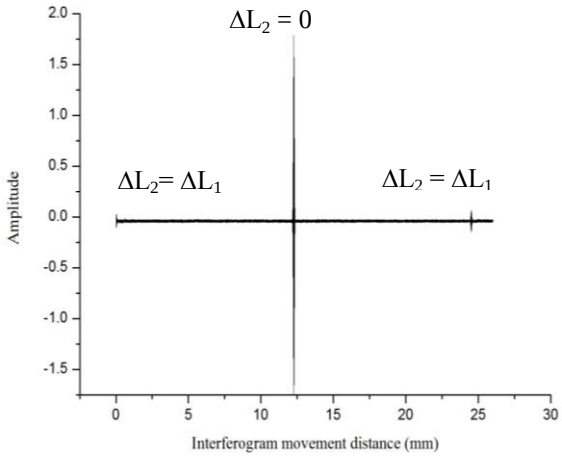

Figure 3. Optical intensity relative to the movable collimator position.

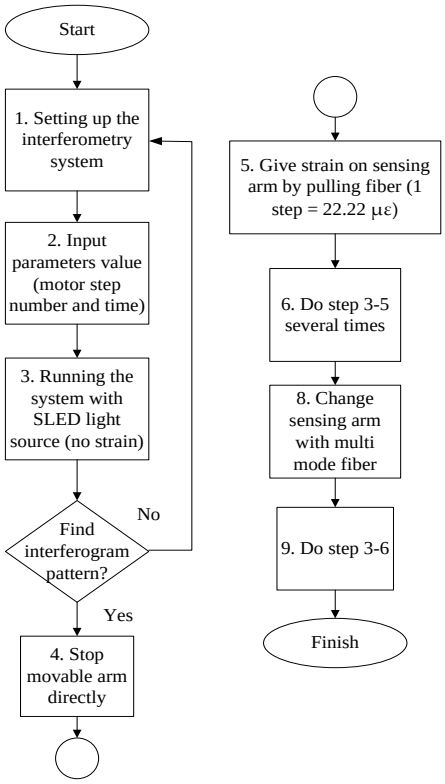

Figure 4. Flow Chart of the Experiment.

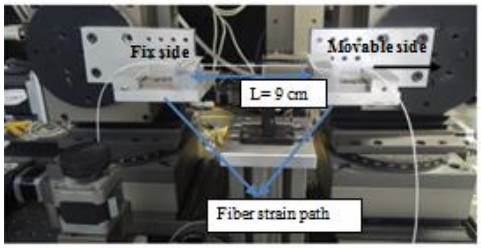

Figure 5. Sensing Arm of the MZ Interferometry.

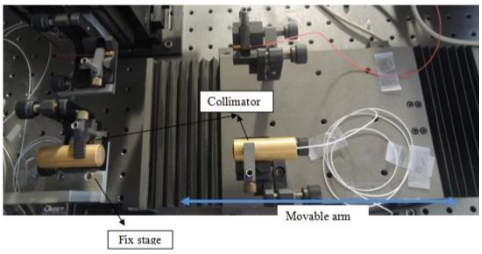

Figure 6. Movable arm of the MZ interferometry.

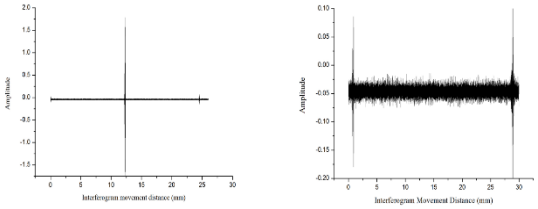

(a) (b)

Figure 7. Interferogram Pattern of MZ interferometry with sensing arm; (a) SMF; (b) MMF

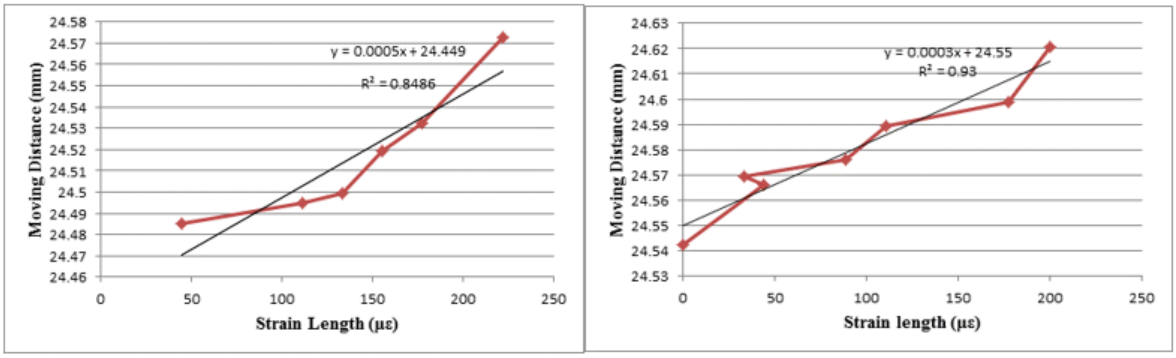

(a) (b)

Figure 8. Fiber strain characterization of single mode fiber (a) first measurement; (b) second measurement.

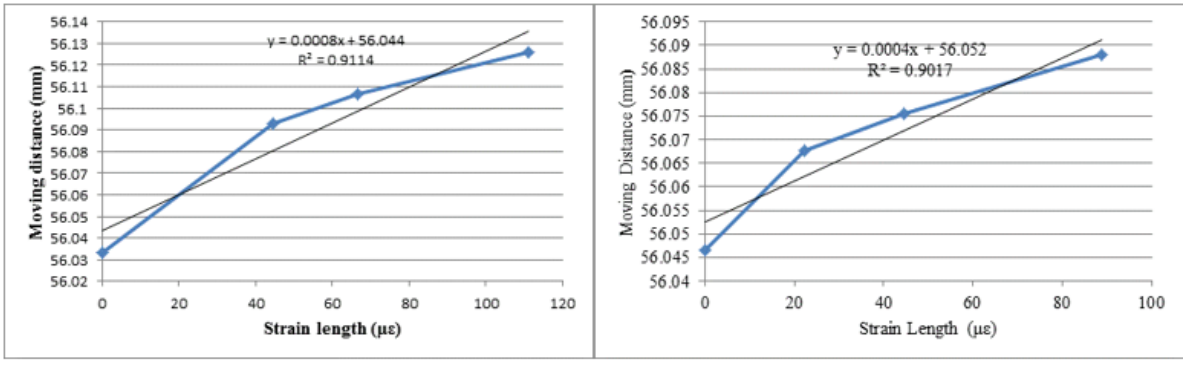

(a) (b)

Figure 9. Strain characterization of multimode fiber (a) first measurement; (b) second measurement